RAPID COMMUNICATIONS

PHYSICAL REVIEW B VOLUME 43, NUMBER 17 15 JUNE 1991-I

Local-density functional photoelectron spectra of fullerenes

J. W. Mintmire, B. I. Dunlap, D. W. Brenner, R. C. Mowrey, and C. T. White
Naval Research Laboratory, Washington, D.C. 20375-5000
(Received 27 February 1991)

We have calculated the electronic structure of several hollow-carbon-cage molecules—the "fullerenes"—via an all-electron Gaussian-orbital-based local-density-functional approach. Starting with the one-electron wave functions and eigenvalues obtained from these calculations, we have further calculated spherically averaged cross sections for photoelectron emission, using a first-order time-dependent perturbation-theory approach. We present results for C_{60} (the sixty-atom molecule with truncated-pentagonal-icosahedron structure), C_{70}, and C_{84}, and compare these theoretical predictions with recent experimental results for C_{60}.

Recently developed synthetic techniques have isolated and purified macroscopic amounts of a series of materials believed to be formed from structures of all-carbon hollow-cage clusters.[1] At least three such cluster materials have been prepared and isolated: C_{60}, C_{70}, and C_{84}.[1-7] Nuclear magnetic resonance results[2-4] support the suggestion of Kroto *et al.*,[8] that the building blocks of these materials are high-symmetry cage structures, with C_{60} having the highly-symmetric truncated-pentagonal-icosahedron shape. Together with other related cage molecules, it belongs to a family of molecules called the "fullerenes." With the production of macroscopic amounts of these cluster materials, valence photoelectron spectroscopic measurements are now becoming available.[9,10]

We have previously calculated the electronic structure and total energy, and consequently optimized the equilibrium geometry of C_{60} and hydrogenated and fluorinated C_{60} systems[11,12] using a Gaussian-orbital-based local-density-functional (LDF) approach.[13,14] We have also shown that a good theoretical estimate of photoelectron line shapes can be calculated from such electronic-structure results.[15,16] This method uses time-dependent perturbation theory to evaluate the spherically-averaged cross sections for transitions from the LDF one-electron wave functions to an outgoing plane-wave state. Herein we apply this approach to the fullerenes C_{60}, C_{70}, and C_{84}, and compare our theoretical cross sections with reported results for thin films of C_{60}.

We use our LDF electronic structure results in conjunction with an approach[17-19] long established to estimate photoelectron cross sections for small molecules. First-order time-dependent perturbation theory and a semiclassical description of the radiation-matter interaction are used to calculate the cross sections necessary to describe the photoelectron spectra. Within this approach, the differential cross section for bound-to-free transitions from an initial state, u_i, to a final state, u_f, induced by incident radiation of energy $\hbar\omega$ and averaged over polarization and direction of incidence is proportional to $|\mathbf{P}_{i\to f}|^2$, where $\mathbf{P}_{i\to f}$ is the transition matrix element defined by[20]

$$\mathbf{P}_{i\to f} = \int d^3r\, u_f(\mathbf{r})\nabla u_i(\mathbf{r}) \ . \tag{1}$$

Following earlier workers,[17-19] we approximate the final outgoing state u_f with a plane wave having outgoing momentum $\hbar\mathbf{k}_f$. This final-state wave vector $\mathbf{k}_f$ must conserve total energy such that $\hbar^2k_f^2/2m = \hbar\omega + \varepsilon_i$, where ε_i is the energy of the one-electron initial state u_i. Using the above equations and the anti-Hermitian nature of the gradient operator, we can evaluate $\mathbf{P}_{i\to f}$ as a term proportional to the overlap between the occupied one-electron wave function $u_i(\mathbf{r})$ calculated using our LDF approach, and the outgoing plane wave, $\exp(i\mathbf{k}_f\cdot\mathbf{r})$. Typically, experimental photoelectron spectra are not angularly resolved and thus produce averages over all allowed orientations of the outgoing wave vector. We therefore spherically average the transition probability as described in our earlier work.[15,16] Although the plane-wave approximation will be better far from threshold and hence better for x-ray photoemission spectroscopy (XPS) than ultraviolet photoemission spectroscopy (UPS), we generally find good agreement between theory and experiment for both XPS and UPS in previous systems studied.

We calculate the LDF electronic structure using molecular orbitals constructed from linear combinations of Gaussian-type functions. Within this approach the electron repulsion and exchange-correlation potentials are evaluated using a variational fitting of the charge density[13,21] and orbital and potential fitting basis sets constructed from products of solid-spherical harmonics and Gaussian functions.[22] Maximal use of symmetry has been incorporated into a computer code[14] capable of calculating both the total energy as well as the one-electron energies and wave functions. The LDF used herein is the Perdew-Zunger[23] fit of the free-electron-gas results of Ceperley and Alder.[24]

We have found the LDF equilibrium geometry (for an

$11s7p1d$ carbon orbital basis set) for C_{60} in I_h symmetry by minimizing the LDF total energy as a function of the two independent bond lengths,[25] with resulting bond lengths of 1.39 and 1.45 Å. We have calculated spherically-averaged photoelectron cross sections for the resulting one-electron states for a series of incident photon energies: 40.8, 65.0, 170.0, and 1486.6 eV. Table I presents our predicted photoelectron intensities for C_{60} for the occupied valence states of C_{60}, and also gives the symmetry and LDF one-electron eigenvalue of each state. The intensities listed are the product of the calculated transition probability and the corresponding occupation number for the one-electron state, and have been scaled so that the maximum intensity for the valence states is unity. As is typical in photoelectron spectra, the location of the most intense peaks shifts to more strongly bound states with increasing incident photon energy.

Lichtenberger *et al.*[9] have recently reported photoelectron spectroscopy results for C_{60} at 21.2 and 40.8 eV.

TABLE I. Relative theoretical photoelectron intensities for LDF one-electron states of C_{60}, for various photon energies $\hbar\omega$. One-electron eigenvalues are relative to HOMO value of −5.94 eV.

State	Electronic energy (eV)	Relative intensity at photon energy $\hbar\omega$ (eV) 40.8	65.0	170.0	1486.6
$6h_u$	0.00	1.00	0.80	0.74	0.01
$6g_g$	−1.18	0.73	0.59	0.55	0.01
$10h_g$	−1.30	0.92	0.73	0.67	0.01
$5h_u$	−2.83	1.00	1.00	1.00	0.02
$6g_u$	−2.89	0.66	0.53	0.49	0.01
$9h_g$	−3.14	0.95	0.95	0.96	0.06
$6t_{2u}$	−3.44	0.47	0.39	0.36	0.01
$5g_u$	−4.16	0.75	0.77	0.79	0.05
$2t_{2g}$	−4.63	0.50	0.49	0.51	0.12
$8h_g$	−4.76	0.70	0.60	0.55	0.03
$5g_g$	−4.91	0.63	0.66	0.71	0.18
$7h_g$	−5.31	0.85	0.89	0.91	0.09
$4g_u$	−5.81	0.60	0.60	0.62	0.17
$6t_{1u}$	−5.90	0.37	0.33	0.31	0.02
$4a_g$	−6.50	0.11	0.10	0.10	0.01
$5t_{2u}$	−6.53	0.43	0.46	0.48	0.08
$5t_{1u}$	−7.11	0.41	0.44	0.47	0.13
$4h_u$	−7.31	0.53	0.55	0.68	0.58
$4g_g$	−8.12	0.46	0.48	0.53	0.26
$3a_g$	−9.40	0.13	0.15	0.15	0.00
$2t_{1g}$	−9.53	0.22	0.21	0.32	0.50
$6h_g$	−9.76	0.42	0.46	0.60	0.62
$4t_{2u}$	−10.85	0.28	0.30	0.34	0.25
$4t_{1u}$	−11.84	0.23	0.24	0.31	0.36
$3h_u$	−11.95	0.25	0.21	0.43	1.00
$3g_g$	−13.48	0.22	0.17	0.32	0.72
$5h_g$	−13.96	0.24	0.23	0.40	0.84
$3g_u$	−15.24	0.34	0.13	0.27	0.73
$3t_{2u}$	−16.08	0.10	0.09	0.20	0.54
$4h_g$	−17.10	0.13	0.10	0.29	0.95
$3t_{1u}$	−18.08	0.06	0.04	0.16	0.58
$2a_g$	−18.59	0.02	0.01	0.05	0.19

To compare with these and other[10] results, we depict our predicted photoelectron line shapes for incident photoelectron energies of 40.8 and 1486.6 eV in Fig. 1, as well as the experimental UPS He II spectra of Ref. 9. In this figure we plot a photoelectron line shape constructed by broadening our predicted line spectra with a 0.4-eV-wide at half-maximum Gaussian function. The relative intensities in both curves have been scaled to yield identical maximum values. Our highest-occupied molecular orbital (HOMO) one-electron eigenvalue would predict a first vertical ionization potential (IP) of 5.94 eV, slightly less than the reported IP of 7.6 eV.[9] Our calculated one-electron energies relative to the HOMO threshold, however, agree closely with the experimental results. Our relative intensities are also in good agreement, especially considering that the plane-wave approximation made in our calculations will be worst for this UPS case.[26]

Lichtenberger *et al.*[9] point out five major features on their reported photoelectron spectra. The first feature, at threshold, they assign to a transition from an h_u state. The second, down roughly 1.35 eV from threshold, they assign to a double transition from g_g and h_g states. As can be seen in Table I, our one-electron results support this assignment. Lichtenberger *et al.*[9] find that the relative intensities of these two peaks are nearly equal, in contrast to the expected ratio of second to first peak intensities of 18:10 expected from their respective electron occupations. Our cross sections predict a slightly smaller ratio of roughly 16:10, but do not predict a decrease to roughly 1:1. This feature might result from the above-mentioned limitations of the plane-wave approximation in UPS spectra. Indeed, Weaver *et al.*,[10] reporting pho-

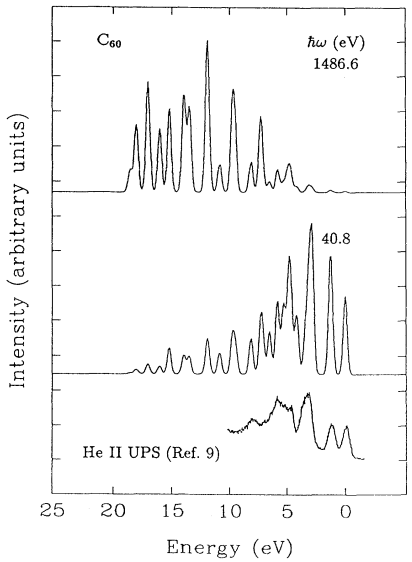

FIG. 1. Theoretical photoelectron line shapes from LDF results for C_{60} at incident photon energies of 40.8 and 1486.6 eV. One-electron energies are relative to the HOMO level (−5.94 eV). Bottom curve depicts experimental He II UPS spectra of Ref. 9.

toelectron spectra of C_{60} for photon energies from 40.0 to 1486.6 eV, indicate that this ratio of peak heights oscillates markedly as the incident photon energy is varied from 40 to 65 eV.

The rest of our predicted line shape appears in excellent agreement with the UPS experimental results.[9,10] Lichtenberger *et al.*[9] report a third peak roughly 3.2–4.0 eV down from threshold which they tentatively assign to transitions from g_u and t_{2u} states. Our results suggest that this feature also includes transitions from h_u and h_g states. Two additional broad features are reported at roughly 5–6 and 8 eV down from threshold with no assignments attempted. Our results suggest that the fourth feature can be assigned to a combination of seven transitions from the following states: $5g_u$, $2t_{2g}$, $8h_g$, $5g_g$, $7h_g$, $4g_u$, and $6t_{1u}$. The fifth feature can be assigned to a combination of five transitions from the following states: $4a_g$, $5t_{2u}$, $5t_{1u}$, $4h_u$, and $4g_g$.

Weaver *et al.*[10] report similar results using a synchrotron source to produce photoelectron spectra for C_{60} over a range of energies. With higher incident photon energies, and resolution typical of synchrotron sources, they discern some additional features over that from the earlier UPS results.[9] First, they discern a low intensity peak intermediate between the fourth and fifth peaks that disappears for incident photon energies above 80 eV. We tentatively assign this peak to transitions from the $4a_g$ and $5t_{2u}$ states, in part because the transition intensity of this peak relative to its immediate neighbors declines as incident photon energy is decreased. Weaver *et al.*[10] also note four additional peaks (their seventh through tenth) in their photoelectron spectra for incident photons with energies of 50 and 65 eV; these peaks are broad and located roughly 11, 12, 15, and 19 eV down from threshold. We would assign this seventh peak to a trio of transitions from the $3a_g$, $2t_{1g}$, and $6h_g$ states, and the eighth peak to a transition from the $4t_{2u}$ state. We would further assign the ninth peak to a pair of transitions from the $4t_{1u}$ and $3h_u$ states, although the broadness of the peaks in the experimental data that deep in the valence region makes a definitive allocation of states between these two final peaks somewhat tentative.

Similar agreement is found between our predicted line shape for XPS (photon energy of 1486.6 eV) and the experimental results.[10] At this high energy we find that the first three peaks in the UPS have become effectively negligible, and the broad fourth peak has become a minor peak. The experimental data at 1486.6 eV indicate four major peaks rising in intensity as the energy shifts further down from threshold, with a final broad background beginning roughly 15 eV from threshold.[10] We find excellent agreement if these four peaks are assigned to the same transitions as we earlier assigned the fourth, sixth, seventh, and ninth peaks, respectively, in the UPS spectra of Weaver *et al.*[10]

We have also carried out similar studies on C_{70} and C_{84}, which have recently been isolated as condensed-phase materials[1–3] in addition to C_{60}. A D_{5h} struc-

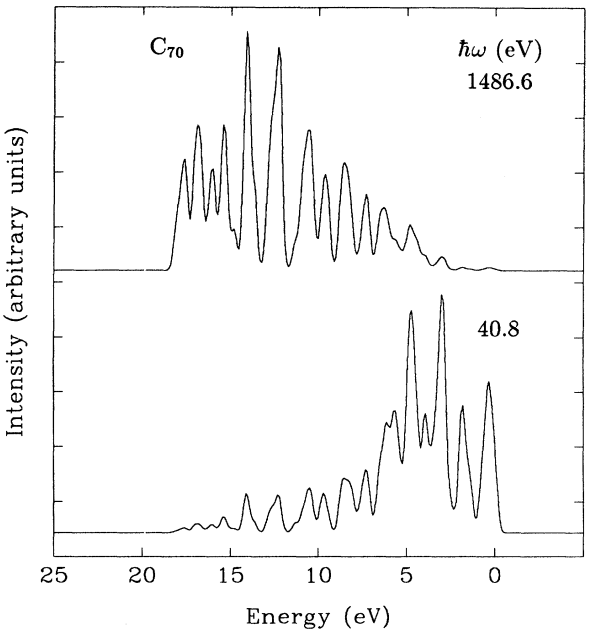

FIG. 2. Theoretical photoelectron line shapes from LDF results for C_{70} at incident photon energies of 40.8 and 1486.6 eV. One-electron energies are relative to the HOMO level (−5.99 eV).

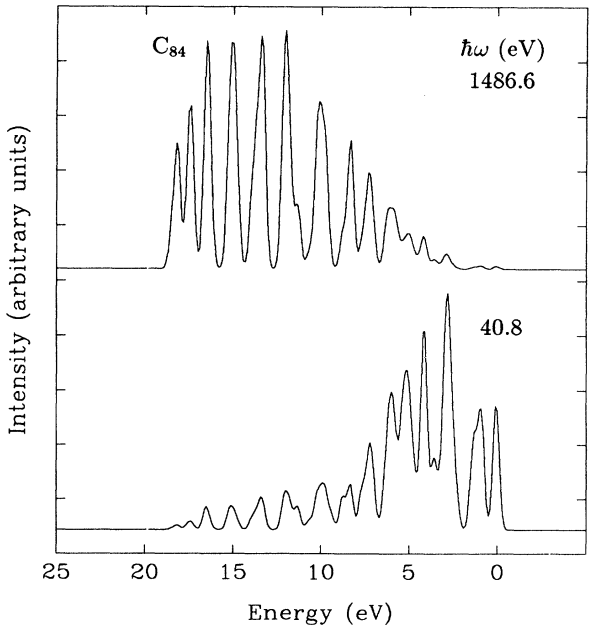

FIG. 3. Theoretical photoelectron line shapes from LDF results for C_{84} at incident photon energies of 40.8 and 1486.6 eV. One-electron energies are relative to the HOMO level (−5.88 eV).

ture was used for C_{70} and a T_d structure was used for C_{84}, as suggested by recent model studies.[27,28] Because these two molecules have several more degrees of freedom than C_{60}, we first found an optimized geometry using a recently developed empirical potential for hydrocarbons.[29] Our equilibrium geometry for C_{70} has carbon-carbon bond lengths ranging from 1.43 to 1.49 Å, and our equilibrium geometry for C_{84} has carbon-carbon bond lengths ranging from 1.38 to 1.45 Å. Full details of these calculations will be reported elsewhere.[25] LDF calculations were then performed for the equilibrium geometries obtained, and photoelectron cross sections were calculated. We depict our predictions for the photoelectron line shapes (again broadened with a 0.4-eV-wide Gaussian function) resulting from incident photon energies of 40.8 and 1486.6 eV for C_{70} in Fig. 2 and for C_{84} in Fig. 3.

We note that the breaking of the C_{60} I_h symmetry (to D_{5h} in C_{70} and T_d in C_{84}) leads to a broadening of the expected photoelectron line shapes relative to the C_{60} spectra. In particular, we expect the UPS spectra to have only two sharp peaks near threshold, rather than the three observed in C_{60}. Rather than the sharp peak at threshold arising from a single transition observed in C_{60}, we expect a broad transition arising from twenty valence electrons in five states ($19e_1''$, $14a_2''$, $7a_2'$, $19e_2''$, $23e_2'$, and $23e_1'$) as the first UPS peak for C_{70}. Our one-electron eigenvalues are contained in a 0.7-eV interval; the experimental line would have additional instrumental broadening. Similarly, the first peak in C_{84} arises from transitions from three states ($22e$, $27t_1$, and $7a_2$) within 0.1 eV of each other.

In summary, we have performed local-density functional electronic structure calculations on the I_h conformation proposed for C_{60} and further calculated spherically-averaged photoelectron cross sections for the one-electron states. We find excellent agreement between reported experimental results of the photoelectron spectra of thin films of a recently synthesized C_{60} cluster material.[9,10] This agreement strongly supports current beliefs that the material is comprised of a structure of icosahedral C_{60} clusters with minimal electronic interaction between clusters. We have also calculated electronic structures and photoelectron cross sections for the other two materials recently isolated and purified—C_{70} and C_{84}—for which as yet no photoelectron spectra have been reported. However, our results for these two materials will be useful in determining whether their C_{70} and C_{84} building blocks remain intact in the condensed-phase material and have the D_{5h} and T_d structures earlier suggested[27,28] and used as starting points in our calculations.

This work was supported in part by the U.S. Office of Naval Research under Contract No. N00014-91-WX-24154. Computational support for this project was provided in part by a grant of computer resources from the Naval Research Laboratory.

[1] W. Krätschmer *et al.*, Chem. Phys. Lett. **170**, 167 (1990); Nature **347**, 354 (1990).
[2] R. Taylor *et al.*, J. Chem. Soc., Chem. Commun. **1990**, 1423.
[3] R. D. Johnson, G. Meijer, and D. S. Bethune, J. Am. Chem. Soc. **112**, 8983 (1990).
[4] H. Ajie *et al.*, J. Phys. Chem. **94**, 8630 (1990).
[5] R. E. Haufler *et al.*, J. Phys. Chem. **94**, 8634 (1990).
[6] J. W. Arbogast *et al.*, J. Phys. Chem. **95**, 11 (1991).
[7] J. M. Hawkins *et al.*, J. Org. Chem. **55**, 6250 (1990).
[8] H. W. Kroto *et al.*, Nature **318**, 162 (1985).
[9] D. L. Lichtenberger *et al.*, Chem. Phys. Lett. **176**, 203 (1991).
[10] J. H. Weaver *et al.*, Phys. Rev. Lett. **66**, 1741 (1991).
[11] B. I. Dunlap, Int. J. Quantum Chem. Symp. **22**, 257 (1988).
[12] B. I. Dunlap *et al.*, J. Phys. Chem. (to be published); B. I. Dunlap *et al.*, in *Clusters and Cluster-Assembled Materials*, edited by R. S. Averback, D. L. Nelson, and J. Bernhole, MRS Symposia Proceedings No. 206 (Materials Research Society, Pittsburgh, 1991).
[13] B. I. Dunlap, J. W. D. Connolly, and J. R. Sabin, J. Chem. Phys. **71**, 3396 (1979); **71**, 4993 (1979).
[14] B. I. Dunlap and N. Rösch, in *Advances in Quantum Chemistry*, edited by S. B. Trickey (Academic, New York, 1990), p. 317.
[15] J. W. Mintmire and C. T. White, Int. J. Quantum Chem. Symp. **17**, 609 (1983).
[16] J. W. Mintmire, F. W. Kutzler, and C. T. White, Phys. Rev. B **36**, 3312 (1987).
[17] S. Basu, Theor. Chim. Acta (Berlin) **3**, 238 (1965).
[18] I. G. Kaplan and A. P. Markin, Opt. Spektrosk. **24**, 884 (1968) [Opt. Spectrosc. (USSR) **24**, 475 (1968)].
[19] L. L. Lohr, Jr. and M. B. Robin, J. Am. Chem. Soc. **92**, 724 (1970).
[20] K. Smith, *The Calculation of Atomic Collision Processes* (Wiley-Interscience, New York, 1971).
[21] J. W. Mintmire and B. I. Dunlap, Phys. Rev. A **25**, 88 (1982).
[22] B. I. Dunlap, Phys. Rev. A **42**, 1127 (1990).
[23] J. P. Perdew and A. Zunger, Phys. Rev. B **23**, 5948 (1980).
[24] D. M. Ceperley and B. J. Alder, Phys. Rev. Lett. **45**, 566 (1980).
[25] B. I. Dunlap *et al.* (unpublished).
[26] For incident photons of 40.8 eV energy, the outgoing plane wave for an excitation from the HOMO has a wavelength of roughly 2 Å. For such an outgoing electron state only ~ 30 eV into the continuum and with a wavelength slightly larger than the carbon-carbon nearest-neighbor distances, we could expect discernible effects on the transition cross sections arising from modulation of the outgoing electron state by the molecular potential.
[27] T. G. Schmalz *et al.*, J. Am. Chem. Soc. **110**, 1113 (1988).
[28] R. L. Whetten (private communication).
[29] D. W. Brenner, Phys. Rev. B **42**, 9458 (1990).